Modulating Biological Rhythms: A Noncomputational Strategy Harnessing Nonlinearity and Decoupling Frequency and Amplitude

Zhaoyue Zhong (仲昭月),[1] Wei Lin (林伟),[1,2,3,4,*] and Bo-Wei Qin (秦伯韡)[2,3,4,†]
[1]School of Mathematical Sciences and Shanghai Center for Mathematical Sciences, Fudan University, 200433 Shanghai, China
[2]Research Institute of Intelligent Complex Systems, Fudan University, 200433 Shanghai, China
[3]Shanghai Artificial Intelligence Laboratory, 200232 Shanghai, China
[4]State Key Laboratory of Medical Neurobiology and MOE Frontiers Center for Brain Science, Institute of Brain Science, Fudan University, 200032 Shanghai, China

(Received 14 February 2023; revised 17 July 2023; accepted 30 August 2023; published 29 September 2023)

Understanding and achieving concurrent modulation of amplitude and frequency, particularly adjusting one quantity and simultaneously sustaining the other at an invariant level, are of paramount importance for complex biophysical systems, including the signal pathway where different frequency indicates different upstream signal yielding a certain downstream physiological function while different amplitude further determines different efficacy of a downstream output. However, such modulators with clearly described and universally valid mechanisms are still lacking. Here, we rigorously propose an easy-to-use control strategy containing only one or two steps, leveraging the nonlinearity in the modulated systems to decouple frequency and amplitude in a noncomputational manner. The strategy's efficacy is demonstrated using representative biochemical systems and, thus, it could be potentially applicable to modulating rhythms in experiments of biochemistry and synthetic biology.

DOI: 10.1103/PhysRevLett.131.138401

Biological rhythms are prominently characterized by frequency and amplitude [1,2]. Their precise quantities are crucial to signal transduction, homeostatic maintenance, and life health [3–5], whereas their disorders may cause detrimental consequences [6,7]. Therefore, tuning the two quantities appropriately and unraveling intrinsic mechanisms accurately become challenging issues that have been investigated mostly using dynamical systems tools [8–12]. Many works explored the roles of internal autoregulation [13–15]. Besides, the significance of independent amplitude modulation (IAM) and independent frequency modulation (IFM) for a number of typical biophysical models were discussed and analyzed numerically [16,17]. Both independent modulations are fundamental and critical because achieving them implies tunability in biorhythm regulation. They were recently realized in specific models by redesigning biological circuitry in a brute-force manner without theoretical illumination [18,19].

Oscillations stemming from the Hopf bifurcation are pervasive in biophysical context [20–22]. The Kuramoto model is a remarkable example derived from the normal form of this bifurcation for studying synchronization of coupled oscillators with immobile amplitude [23]. A generic dynamical system, which describes the emergent biological rhythms from the Hopf bifurcation, reads

$$\dot{\boldsymbol{x}} = \boldsymbol{f}(\boldsymbol{x}, \alpha), \qquad \boldsymbol{x} \in \mathbb{R}^n, \tag{1}$$

where $\boldsymbol{x} = [x_1, \ldots, x_n]^\top$, and $\alpha \in \mathbb{R}$ is a bifurcation parameter which is typically an internal or external signal of biological significance. The steady state $\boldsymbol{x}_{\rm ss}$ undergoes the Hopf bifurcation at $\alpha = \alpha^*$ yielding a stable oscillation. To analyze its amplitude and frequency, we generally find below the expression in terms of $\boldsymbol{y} = \boldsymbol{x} - \boldsymbol{x}_{\rm ss}$,

$$\dot{\boldsymbol{y}} = \boldsymbol{J}(\alpha)\boldsymbol{y} + \boldsymbol{G}(\boldsymbol{y}; \alpha) + \mathcal{O}(\|\boldsymbol{y}\|^4), \qquad \boldsymbol{y} \in \mathbb{R}^n, \tag{2}$$

where the linear interactions are described by the *Jacobian* matrix $\boldsymbol{J} = \{J_{ij}\}$ and the nonlinear ones the term $\boldsymbol{G}(\boldsymbol{y}; \alpha)$, whose kth element follows $G_k(\boldsymbol{y}; \alpha) = \sum_{2 \le i_1 + \cdots + i_n \le 3}^{i_1, \ldots, i_n \ge 0} [g_k^{(i_1 \ldots i_n)}(\alpha) y_1^{i_1} \ldots y_n^{i_n}]$. The *Jacobian* matrix $\boldsymbol{J}$ has a pair of eigenvalues $\lambda_{1,2} = \mu(\alpha) \pm i\omega(\alpha)$ corresponding to the Hopf bifurcation. The eigenvector associated with λ_1 is denoted by $\boldsymbol{q} \in \mathbb{C}^n$ which, as we will see, is significant for quantifying the amplitude.

Lately, IAM and IFM were achieved in Eq. (1) by using different linear feedback controllers $\boldsymbol{u} = \boldsymbol{F}\boldsymbol{y}$ [24,25], see Fig. 1(a) for a schematic diagram when $n = 2$. For each system to be modulated, $\boldsymbol{F} = \{f_{ij}\}$ could be predicted precisely through computing the normal form, whereby the amplitude and frequency can be quantified [26]. However, computation of the normal form is often a complicated and experimentally unfriendly task, especially for complex systems of high-dimension [27] which, thus, impedes a real and even broad application of the developed control

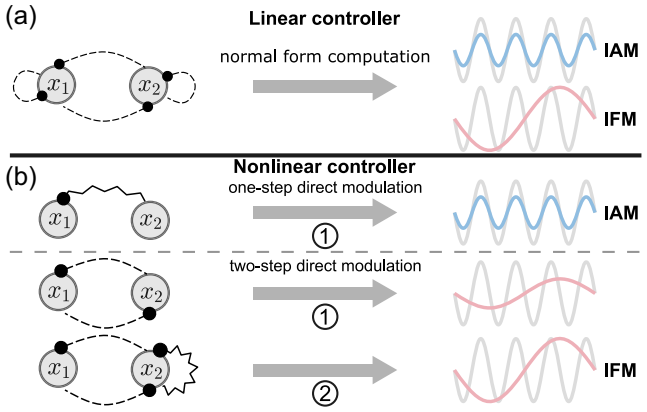

FIG. 1. (a) Achieving IAM or IFM by a linear controller requires computing the normal form. (b) Achieving IAM and IFM needs, respectively, one and two steps without computation by harnessing nonlinearity (zigzag) in the controller.

strategy. There is accordingly a high anticipation for designing an easily implemented but still effective approach with less (or even without) computational cost for independent modulations. Such an approach could be a ready-to-use guideline for real experiments.

In this Letter, we rigorously show a constructive role of an appropriate form of the controller $\boldsymbol{u}$ harnessing nonlinearity in decoupling the frequency and the amplitude, which has not been fully considered in the previous studies. By leveraging this unique feature, we design a universal strategy to accomplish IAM and IFM directly and efficiently [Fig. 1(b)]. Though its principle is established by using the normal form, it can be practically implemented using very little knowledge of dynamical systems and even less computational effort. Its practical usefulness is also validated in complex biophysical systems or networks of high or even infinite dimension.

Theory in general.—First, we demonstrate how the amplitude as well as the frequency is quantified using the normal form for designing an effective controller. For system (1), its normal form undergoing the Hopf bifurcation, by standard invertible coordinate changes [see [26] and Supplemental Material (SM), Sec. 1 [28] for detailed procedures], is obtained as

$$\dot{z} = (\mu \pm i\omega)z + \eta z^2\bar{z} + \mathcal{O}(\|z\|^4), \qquad z \in \mathbb{C}, \tag{3}$$

where $\eta \in \mathbb{C}$, and $\chi := \Re(\eta)$ is the first Lyapunov coefficient. Thus, we have the following proposition.

Proposition 1.—In system (3), μ and ω depend only on J_{ij}, while χ depends on both J_{ij} and $g_k^{(i_1 \ldots i_n)}$. So, we can write $\mu = \mu(J_{ij})$, $\omega = \omega(J_{ij})$, and $\chi = \chi(J_{ij}, g_k^{(i_1 \ldots i_n)})$.

Although system (3) has a limit cycle whose frequency and amplitude are calculated, by considering the terms up to the third order, as $F = \omega/2\pi$ and $A = 2\sqrt{-\mu/\chi}$, this cycle actually is a projection of the original periodic orbit that we desire to control in n-dimensional space [26]. Thus, we establish a correspondence between these two orbits. Precisely, the frequency and the amplitude of each component x_i, denoted, respectively, by F_i and A_i, follow the theorem below (proved in SM, Sec. 1 [28]).

Theorem 1.—In system (1), the frequency and the amplitude of x_i, corresponding to the periodic orbit aroused by the Hopf bifurcation, can be calculated, respectively, as $F_i = F = \omega/2\pi$ and $A_i = 4\|q_i\|\sqrt{-\mu/\chi}$, where q_i is the ith element of the eigenvector $\boldsymbol{q}$.

With this, we now briefly review the efficacy as well as the limitation of the linear controller $\boldsymbol{u} = \boldsymbol{F}\boldsymbol{y}$ [25], before proposing a nonlinear one. The controller should satisfy the *bifurcation-* and the *scale-invariance* conditions. The former one ensures the invariant critical parameter α^* for the Hopf bifurcation, while the latter one guarantees that all amplitudes change consistently, i.e., A_i/A_j is static for all i, j. The linear controller is indeed a perturbation made on the *Jacobian* matrix $\boldsymbol{J}$. Therefore, by Proposition 1 and Theorem 1, an undesigned linear controller may change the frequency and the amplitude simultaneously. Computing the normal form is thus unavoidable for decoupling the two quantities, which is necessary for achieving IAM and IFM. However, it may not be an easy task [27] especially for high-dimensional systems (refer to the tedious computation shown in SM, Secs. 1 and 2 [28]).

To overcome this limitation, we here propose a controller harnessing nonlinearity which is underappreciated before. Specifically, we design it as a perturbation in only the nonlinear coefficients $g_k^{(i_1 \ldots i_n)}$. Rigorously, such a controller satisfies

$$\boldsymbol{u} = \mathcal{O}(\|\boldsymbol{y}\|^2) \quad \text{or} \quad \boldsymbol{u} = \mathcal{O}(\|\boldsymbol{y}\|^3), \tag{4}$$

which follows the theorem below (proved in SM, Sec. 3 [28]).

Theorem 2.—If a controller to system (1) is designed as (4), then (i) the frequency F of the periodic orbit aroused by the Hopf bifurcation remains static, whereas the amplitudes A_i changes, and (ii) the *bifurcation-* and the *scale-invariance* conditions are valid.

We therefore approach a surprising conclusion that, for system (1), any controller that regulates only nonlinear terms can decouple the frequency and the amplitude spontaneously. This conclusion suggests that computing the normal form explicitly is unnecessary for independent modulations, though we later compute them tediously in several examples and use Theorem 1 to validate our rigorous findings.

With the uncovered *spontaneous-decoupling* mechanism, we are ready to design specific controllers for IAM. According to Theorem 2, the only requirement is to design a controller $\boldsymbol{u}$ with biologically plausible form that satisfies the form described in (4). As we will see later,

this can be achieved in representative biophysical systems, including the gene regulatory and the neuronal oscillators.

Compared with IAM, achieving IFM is a more complicated task because altering the frequency must require a linear controller, which also changes the amplitude without delicate design (computing the normal form explicitly). Thanks to Theorem 2, we can now propose a two-step strategy [Fig. 1(b)] without tedious computation.

Step 1: Applying a linear controller $\boldsymbol{u} = \boldsymbol{L}(\Delta\omega)\boldsymbol{y}$, with $\boldsymbol{L} \in \mathbb{R}^{n\times n}$, satisfying the *bifurcation-* and *scale-invariance* conditions to change the frequency by $\Delta\omega/(2\pi)$. Though the frequency is modulated, the amplitude deviates from the original level (Proposition 1 and Theorem 1). A recovery step is therefore needed.

Step 2: Designing a nonlinear controller satisfying Eq. (4) to restore the amplitude. According to Theorem 2, the frequency remains as $(\omega + \Delta\omega)/(2\pi)$. Therefore, an oscillation with modulated frequency and static amplitude is eventually obtained. The following theorem guarantees the existence of the control matrix $\boldsymbol{L}$ used in Step 1, where we also provide a specific design for system (1) when $n = 2$. See SM, Sec. 4 [28] for its proof and the design of $\boldsymbol{L}$ when $n > 2$.

Theorem 3.—Assume that $\Re(q_i)\Im(q_j) \neq \Re(q_j)\Im(q_i)$ for any $i \neq j$. Then, there exists a matrix $\boldsymbol{L} = \{\ell_{ij}(\Delta\omega)\} \in \mathbb{R}^{n\times n}$, with at most $2n$ nonzero elements, such that, if the controller $\boldsymbol{u} = \boldsymbol{L}\boldsymbol{y}$ is applied to system (1), then the frequency F of the periodic orbit aroused by the Hopf bifurcation becomes $(\omega + \Delta\omega)/(2\pi)$. Moreover, $\boldsymbol{u}$ satisfies the *bifurcation-* and the *scale-invariance* conditions. Specifically, when $n = 2$, $\ell_{11} = \ell_{22} = 0$, $\ell_{12} = aJ_{12}$, and $\ell_{21} = aJ_{21}$, where $a = \sqrt{1 - (2\omega\Delta\omega + \Delta\omega^2)/(J_{12}J_{21})} - 1$.

We remark that the condition used in Theorem 3 is a common case for applications. Specifically, it is satisfied for all examples considered in the present work. Moreover, $|\Delta\omega|$ cannot be arbitrarily large, because it may change the sign of the first Lyapunov coefficient χ, which makes the periodic orbit unstable. Generally, the feasible range of $\Delta\omega$ is mathematically nonempty but could be determined numerically.

Note that the design of $\boldsymbol{L}$ in Theorem 3 does not require computing the normal form. We only need to do basic linear algebra (see SM, Sec. 4 [28]). In light of Theorems 2 and 3, we have now proposed a one-step (respectively, two-step) control strategy harnessing nonlinearity for IAM (respectively, IFM) in a noncomputational manner. Practical application therefore does not require an understanding of the center manifold or the normal form theories, however, they are essential for validating our results.

Demonstration in a genetic oscillator.—To validate the efficacy of the nonlinear controller and compare it with a linear one in the form of $\boldsymbol{u} = \boldsymbol{F}\boldsymbol{y}$, we first consider a representative genetic oscillator describing the interaction between mRNA (X) and associated protein (Y) [29],

$$\begin{aligned}\dot{X} &= k_1 S K_d^p/(K_d^p + Y^p) - k_{dx}X,\\ \dot{Y} &= k_{sy}X - k_{dy}Y - k_2 E_T Y/(K_m + Y + K_I Y^2).\end{aligned} \quad (5)$$

This system owns a stable oscillation induced by the Hopf bifurcation (see SM, Sec. 2 [28]). To modulate its amplitude and frequency independently, we first apply the linear controller $\boldsymbol{u} = \boldsymbol{F}\boldsymbol{y}$, where $\boldsymbol{y} = [X - X_{\rm ss}, Y - Y_{\rm ss}]^\top$ with $(X_{\rm ss}, Y_{\rm ss})$ an unstable steady state surrounded by the oscillation. Motivated by a recent biological PID controller [30], $\boldsymbol{u}$ can be generalized as a biologically plausible strategy incorporating the Hill-type function, e.g., $(X - X_{\rm ss})/(k + X - X_{\rm ss}) = \mathcal{O}(|X - X_{\rm ss}|)$ [25]. The results and the prediction (Theorem 1) are presented in Fig. 2(a), where, to measure the variations caused by the control implementation for any concerned variable, we introduce a quantity as $\Gamma_\beta := \beta_c/\beta_0 - 1$ with the variable $\beta \in \{A, F, J_{ij}, \ldots\}$ and $\beta_{c/0}$ taking the respective values in the systems with and without control. Thus, $\Gamma_{A/F}$ represent, respectively, the variations of the amplitude A and the frequency F, and $\Gamma_{J_{ij}} = (J_{ij} + f_{ij})/J_{ij} - 1 = f_{ij}/J_{ij}$ characterizes the variation of any ingredient in $\boldsymbol{J}$. As stated before, designing f_{ij} of a linear controller requires tedious computation of the normal form (see SM, Sec. 2 [28]).

We then design a nonlinear controller as $u(Y) = k_1 \Delta S K_d^p/(K_d^p + Y^p) + \alpha K_1^5/(Y^5 + K_1^5)$ to the first equation of system (5). It combines a perturbation of upstream signal S and an extra Hill-type regulation. Select the parameters particularly as $K_1^5 = Y_{\rm ss}^5/4 + 5K_d^4 Y_{\rm ss}/4$ and $\alpha = -5k_1\Delta S K_d^4/(Y_{\rm ss}^4 + 5K_d^4)$. Then, the controller becomes a simple form of $u(Y) = c(Y - Y_{\rm ss})^2 + \mathcal{O}(|Y - Y_{\rm ss}|^3)$, which satisfies the condition in Theorem 2. Consequently, according to the *spontaneous-decoupling* mechanism, changing the intensity c makes the amplitude independently varied [Fig. 2(b)]. The results are also consistent with the effect of the leading term $(Y - Y_{\rm ss})^2$ and the analytical prediction computed from the normal form and Theorem 1 (SM, Sec. 2 [28]). Outstandingly, we also observe a wider allowable range of the amplitude than that obtained

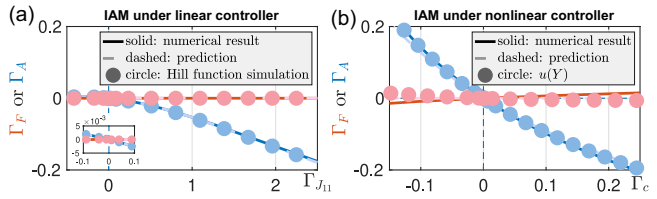

FIG. 2. IAM of system (5) achieved by (a) the linear controller $\boldsymbol{u} = \boldsymbol{F}\boldsymbol{y}$, and (b), the nonlinear controller $c(Y - Yss)^2$ (blue: amplitude; red: frequency). Depictions are the numerical results (solid) and the theoretical predictions obtained by computing the normal form (light dashed). The circles represent the simulated results using the Hill-type function, i.e., $y_j/(y_j + k) \approx y_j$ [25], and the results obtained by using $u(Y)$.

only using the linear controller [Fig. 2(a)]. This discovery deserves a thorough study in the future.

Though the accurate role of the intensity c in $u(Y)$ can be forecast by computing the normal form (Theorem 1), it could be direct to implement $u(Y)$ without prior computation in practice. For a given task, according to Theorem 2, we only need to gradually vary c to achieve IAM. Indeed, the nonlinearity does bring a previously overlooked and mathematically inspired IAM strategy. It actually possesses several hallmarks: it allows a non-computational control, it generates an experimentally friendly approach using one-parameter controller, and it permits a more effective modulation, which allows a wider-tunable range. Apart from applying the quadratic controller $u(Y) = \mathcal{O}(|Y - Y_{ss}|^2)$, using a cubic one $u(Y) = \mathcal{O}(|Y - Y_{ss}|^3)$ is also beneficial to IAM (SM, Sec. 2 [28]).

We also achieve IFM using the above-articulated two-step control strategy to leverage the *spontaneous-decoupling* mechanism induced by the nonlinearity [Figs. 3(a) and 3(b)]. We first apply a linear controller $\boldsymbol{Ly}$ according to Theorem 3 (Step 1), the frequency is thus modulated with undesirable amplitude [Fig. 3(c)]. Then, in light of Theorem 2, we design a nonlinear controller $\boldsymbol{u}(\boldsymbol{y}) = [0, c(Y - Y_{ss})^3]^\top$, which indeed perturbs $g_2^{(03)}$, to complete the entire process of IFM (Step 2). We also observe, from the contour maps, that the range of modulation is enlarged compared with the linear controller (see Fig. S1). Moreover, the required feedback intensities are moderate. Analogous to IAM, the two-step strategy for IFM can be applied without tedious computation because only two control parameters, $\Delta\omega$ and c, are involved. In practice, we first vary $\Delta\omega$ to modulate the frequency. Then alter c to restore the amplitude. This may be achieved as a

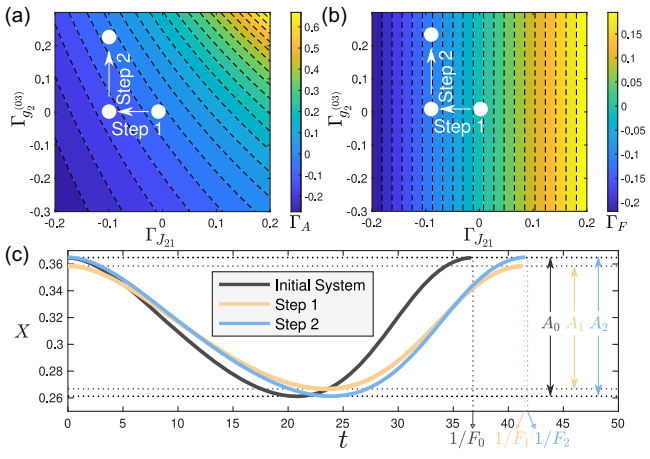

FIG. 3. (a),(b) Variations of the amplitude and the frequency of the oscillation in system (5) under the control strategy harnessing nonlinearity. Dashed lines represent isoamplitude and isofrequency contours. A two-step controller for IFM is highlighted. (c) Three oscillations correspond to the highlighted circles.

controller with two sliders, which is not possible if we adopt the linear controller $\boldsymbol{u} = \boldsymbol{Fy}$ alone. Apparently, this two-step strategy is more practical in applications.

Demonstration in higher-dimensional systems.—We have shown the efficacy and practical usefulness of the nonlinear controller in the two-dimensional genetic oscillator. The strategy is indeed also applicable to systems of higher dimension. We now consider the AC-DC model combining the *toggle switch* and the *repressilator* [31], which sketches the protein-protein interactions: $\dot{x} = f(x, y, z; S)$, $\dot{y} = g(x, y, z; S)$, $\dot{z} = h(x, y, z; S)$ (full model in SM, Sec. 5 [28]). Here, signal S is the chosen bifurcation parameter yielding the Hopf bifurcation [Fig. 4(b)]. To modulate independently the amplitude of the protein concentration, we first implement a biologically plausible controller to regulate the dynamics of protein y which—under appropriate design—satisfies $u(x) = \mathcal{O}(|x - x_{ss}|^2)$ (SM, Sec. 5 [28]). It meets the condition in Theorem 2, and thus helps us achieve IAM (Fig. S4 [28]).

Apart from applying the quadratic controller, a cubic one also exhibits the efficacy and efficiency [Fig. 4(a)]. Additionally, the controller regulating the dynamics of x or z also works (Fig. S5). All the outcomes are well predicted by computing the normal form (SM, Sec. 5), though it is unnecessary to do so in practice. We also validate the efficacy of a fixed controller for oscillations far from the Hopf bifurcation [Figs. 4(b) and 4(c)], where the amplitudes of all proteins are concurrently down regulated indicating that the *scale-invariance* condition holds spontaneously. Additionally, for IFM, we use a two-step control strategy based on Theorems 2 and 3, whose detailed design and the corresponding results are presented in SM, Sec. 5 [28].

Besides genetic or protein dynamics, our control strategy is also helpful for mastering the neurodynamics. Consider the well-known Hodgkin-Huxley neuron model [20], which is usually regarded as a frequency-modulated system. The neurodynamics obey $C\dot{V} = I - \bar{g}_K n^4 (V - E_K) - \bar{g}_{Na} m^3 h (V - E_{Na}) - \bar{g}_L (V - E_L)$,

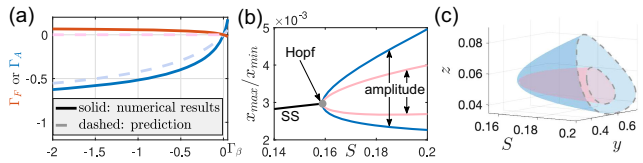

FIG. 4. (a) IAM in the AC-DC model achieved by intervening the nonlinear term [$\beta = g_2^{(300)}$] (solid: numerical result; dashed: theoretical prediction). Under certain intensity, the amplitude (blue) is greatly varied whereas the frequency (red) remains static. (b) Bifurcation diagram with (red) and without (blue) control. The steady state (SS) undergoes the Hopf bifurcation at $S^* \approx 0.1589$. An oscillation arises when $S > S^*$, whose amplitude is altered by the nonlinear controller with $\Gamma_\beta = -1$ (SM S.5). (c) The evolutions of (blue: original; red: controlled) oscillations suggesting that the amplitudes of y and z are also suppressed (dashed cycles: $S = 0.2$).

$\tau(V)\dot{W} = W_\infty(V) - W$, where $W \in \{n, m, h\}$. Following Theorem 2, our computations in SM, Sec. 6 [28] show that an external stimulus satisfying $\Delta I_{\text{in}} = c(V - V_{\text{ss}})^3$ to the membrane potential is sufficient and efficient for realizing IAM.

We further demonstrate the efficacy of the nonlinear controller in an infinite-dimensional system with two variables, which is the reaction-diffusion counterpart of system (5) incorporating the spatial movements of molecules. The two variables thereby become $X(x,t)$ and $Y(x,t)$ whose diffusions are delineated by $d_1\partial^2 X/\partial x^2$ and $d_2\partial^2 Y/\partial x^2$, respectively (full model in SM S.7 [28]). Here, x represents the spatial coordinate. Applying the two-step controller introduced before, we decrease the frequency while the amplitude remains unaltered (Fig. S8). Other tasks (e.g., IFM with higher frequency or IAM) are also achieved by implementing different control intensities or distinct strategies (SM S.7). Though our strategy still works for the infinite-dimensional system, the corresponding mathematical foundation needs to be established in the future, which is beyond the scope of the present work.

As a final example, we show the efficacy of a nonlinear controller satisfying (4) for the Watts-Strogatz [32] neuronal networks with different rewiring probabilities. Leveraging the *spontaneous-decoupling* mechanism in Theorem 2, we successfully modulate independently the amplitudes of the entire population by controlling solely a single neuron (refer to details in SM S.8).

Discussion.—Modulating independently the frequency or the amplitude is a rapidly growing frontier of biophysical control. Before carrying out *in vitro* or *in vivo* experiments, it is necessary and significant to develop a model-based control strategy that is practical enough to be a rigorous guideline. In this Letter, we harness the nonlinearity in its biophysical plausible form for the control design. It may stem from protein multimer and its inhibitory or activatory effects [33], from synaptic interaction in neural dynamics [34], or from high-order interactions [35]. We establish rigorous foundations to support the advantage in nonlinear strategy for modulating biological rhythms. It has the capability of decoupling —in a noncomputational manner—the frequency and the amplitude, which can be leveraged to develop an elementary but effective controller with one or two straightforward steps. A strategy as such can be easily applied showing the potential to help us design experimental schemes.

For a given kinetic model, we can choose any of its variables to design and implement a feasible controller, among which the most effective one may be applied. While only one variable is controlled, all the components are concurrently modulated. This fact enables us to select, in practice, the most accessible one (or the one requiring less or the least consumption and modification).

The strategy proposed here belongs to feedback control that is a promising area in mastering biological dynamics [36,37]. It includes many theoretical and experimental works encompassing stabilizing protein abundance [30], balancing bistability [38], and synchronizing cell cycle [39] with microfluidic devices. Our control strategy is also possible for implementation at these platforms, because the modulation can be achieved without tedious computations.

Though we propose a model-based control strategy, it may also be applied when the model is unknown. Different from using the linear controller for which we need to know the full differential equations to compute the normal form, it is not necessary to do so for the nonlinear controller. The only information we need to acquire is the coordinate of the steady state and the displacement of the oscillation from it. Actually, the steady state could be located by the recently developed methods [40–43]. Our approach can thus be immediately implemented for the data-driven research. Yet, there are further issues that need to be addressed. Particularly, how to modulate an oscillation that is extremely far from the Hopf bifurcation remains challenging.

The authors are grateful to the anonymous reviewers for their constructive comments, which helped us to greatly improve the present work. B.-W. Q. is supported by the STI 2030-Major Projects (Grants No. 2022ZD0208604 and No. 2022ZD0208605), and by the NSFC (Grants No. 12001110 and No. 12371482). W. L. is supported by the NSFC (Grant No. 11925103), by the STCSM (Grants No. 2021SHZDZX0103, No. 22JC1402500, and No. 22JC1401402), and by the SMEC (Grant No. 2023ZKZD04).

*Corresponding author: wlin@fudan.edu.cn
†Corresponding author: boweiqin@fudan.edu.cn

[1] A. S. Coutts and L. Weston, *Cell Cycle Oscillators* (Humana Press, New York, 2016).
[2] J. H. Levine, Y. Lin, and M. B. Elowitz, Functional roles of pulsing in genetic circuits, Science **342**, 1193 (2013).
[3] A. S. Hansen and E. K. O'Shea, Limits on information transduction through amplitude and frequency regulation of transcription factor activity, eLife **4**, e06559 (2015).
[4] F. Rijo-Ferreira and J. S. Takahashi, Genomics of circadian rhythms in health and disease, Genome Med. **11**, 82 (2019).
[5] W. Ruan, X. Yuan, and H. K. Eltzschig, Circadian rhythm as a therapeutic target, Nat. Rev. Drug Discov. **20**, 287 (2021).
[6] J. Bass and J. S. Takahashi, Circadian integration of metabolism and energetics, Science **330**, 1349 (2010).
[7] M. Nassan and A. Videnovic, Circadian rhythms in neurodegenerative disorders, Nat. Rev. Neurol. **18**, 7 (2022).
[8] A. T. Winfree, Biological rhythms and the behavior of populations of coupled oscillators, J. Theor. Biol. **16**, 15 (1967).
[9] J. Hasty, M. Dolnik, V. Rottschäfer, and J. J. Collins, Synthetic Gene Network for Entraining and Amplifying Cellular Oscillations, Phys. Rev. Lett. **88**, 148101 (2002).

[10] Y. Guan, Z. Li, S. Wang, P. M. Barnes, X. Liu, H. Xu, M. Jin, A. P. Liu, and Q. Yang, A robust and tunable mitotic oscillator in artificial cells, eLife **7**, e33549 (2018).
[11] O. Kimchi, C. P. Goodrich, A. Courbet, A. I. Curatolo, N. B. Woodall, D. Baker, and M. P. Brenner, Self-assembly-based posttranslational protein oscillators, Sci. Adv. **6**, eabc 1939 (2020).
[12] J. De Boeck, J. Rombouts, and L. Gelens, A modular approach for modeling the cell cycle based on functional response curves, PLoS Comput. Biol. **17**, e1009008 (2021).
[13] M. De Pittà, V. Volman, H. Levine, G. Pioggia, D. De Rossi, and E. Ben-Jacob, Coexistence of amplitude and frequency modulations in intracellular calcium dynamics, Phys. Rev. E **77**, 030903(R) (2008).
[14] A. Politi, L. D. Gaspers, A. P. Thomas, and T. Höfer, Models of IP3 and Ca2+ oscillations: Frequency encoding and identification of underlying feedbacks, Biophys. J. **90**, 3120 (2006).
[15] Y. J. Joshi, Y. K. Jawale, and C. A. Athale, Modeling the tunability of the dual-feedback genetic oscillator, Phys. Rev. E **101**, 012417 (2020).
[16] T. Y.-C. Tsai, Y. S. Choi, W. Ma, J. R. Pomerening, C. Tang, and J. E. Ferrell, Robust, tunable biological oscillations from interlinked positive and negative feedback loops, Science **321**, 126 (2008).
[17] K. Maeda and H. Kurata, Long negative feedback loop enhances period tunability of biological oscillators, J. Theor. Biol. **440**, 21 (2018).
[18] M. Tomazou, M. Barahona, K. M. Polizzi, and G.-B. Stan, Computational re-design of synthetic genetic oscillators for independent amplitude and frequency modulation, Cell Syst. **6**, 508 (2018).
[19] F. Zhang, Y. Sun, Y. Zhang *et al.*, Independent control of amplitude and period in a synthetic oscillator circuit with modified repressilator, Commun. Biol. **5**, 23 (2022).
[20] E. M. Izhikevich, *Dynamical Systems in Neuroscience: The Geometry of Excitability and Bursting* (MIT Press, Cambridge, MA, 2007).
[21] Y. Murayama, H. Kori, C. Oshima, T. Kondo, H. Iwasaki, and H. Ito, Low temperature nullifies the circadian clock in cyanobacteria through Hopf bifurcation, Proc. Natl. Acad. Sci. U.S.A. **114**, 5641 (2017).
[22] J. J. Tyson and B. Novak, A dynamical paradigm for molecular cell biology, Trends Cell Biol. **30**, 504 (2020).
[23] Y. Kuramoto, Self-entrainment of a population of coupled non-linear oscillators, in: *International Symposium on Mathematical Problems in Theoretical Physics* (Springer, Berlin, Heidelberg, 1975).
[24] T. Ge, X. Tian, J. Kurths, J. Feng, and W. Lin, Achieving modulated oscillations by feedback control, Phys. Rev. E **90**, 022909 (2014).
[25] B.-W. Qin, L. Zhao, and W. Lin, A frequency-amplitude coordinator and its optimal energy consumption for biological oscillators, Nat. Commun. **12**, 5894 (2021).
[26] Y. Kuznetsov, *Elements of Applied Bifurcation Theory* (Springer-Verlag, New York, 2004).
[27] M. Haragus and G. Iooss, *Local Bifurcations, Center Manifolds, and Normal Forms in Infinite-Dimensional Dynamical Systems* (Springer-Verlag, London, 2011).
[28] See Supplemental Material at http://link.aps.org/supplemental/10.1103/PhysRevLett.131.138401 for detailed computation, proofs of theorems, full mathematical models, supplemental results and figures.
[29] B. Novák and J. J. Tyson, Design principles of biochemical oscillators, Natl. Rev. Mol. Cell Biol. **9**, 981 (2008).
[30] M. Chevalier, M. Gómez-Schiavon, A. H. Ng, and H. El-Samad, Design and analysis of a proportional-integral derivative controller with biological molecules, Cell Syst. **9**, 338 (2019).
[31] R. Perez-Carrasco, C. P. Barnes, Y. Schaerli, M. Isalan, J. Briscoe, and K. M. Page, Combining a toggle switch and a repressilator within the AC-DC circuit generates distinct dynamical behaviors, Cell Syst. **6**, 521 (2018).
[32] D. Watts and S. Strogatz, Collective dynamics of 'small-world' networks, Nature (London) **393**, 440 (1998).
[33] N. E. Buchler, U. Gerland, and T. Hwa, Nonlinear protein degradation and the function of genetic circuits, Proc. Natl. Acad. Sci. U.S.A. **102**, 9559 (2005).
[34] A. V. M. Herz, T. Gollisch, C. K. Machens, and D. Jaeger, Modeling single-neuron dynamics and computations: A balance of detail and abstraction, Science **314**, 80 (2006).
[35] H. Mickalide and S. Kuehn, High-order interaction between species inhibits bacterial invasion of a phototroph-predator microbial community, Cell Syst. **9**, 521 (2019).
[36] H. El-Samad, Biological feedback control-respect the loops, Cell Syst. **12**, 477 (2021).
[37] M. H. Khammash, Perfect adaption in biology, Cell Syst. **12**, 509 (2021).
[38] J. B. Lugagne, S. Sosa Carrillo, M. Kirch, A. Köhler, G. Batt, and P. Hersen, Balancing a genetic toggle switch by real-time feedback control and periodic forcing, Nat. Commun. **8**, 1671 (2017).
[39] G. Perrino, S. Napolitano, F. Galdi, A. La Regina, D. Fiore, T. Giuliano, M. di Bernardo, and D. di Bernardo, Automatic synchronisation of the cell cycle in budding yeast through closed-loop feedback control, Nat. Commun. **12**, 2452 (2021).
[40] H. Ma, W. Lin, and Y.-C. Lai, Detecting unstable periodic orbits in high-dimensional chaotic systems from time series: Reconstruction meeting with adaptation, Phys. Rev. E **87**, 050901(R) (2013).
[41] H. Ma, D. W. C. Ho, Y.-C. Lai, and W. Lin, Detection meeting control: Unstable steady states in high-dimensional nonlinear dynamical systems, Phys. Rev. E **92**, 042902 (2015).
[42] Q. Zhu, H. Ma, and W. Lin, Detecting unstable periodic orbits based only on time series: When adaptive delayed feedback control meets reservoir computing, Chaos **29**, 093125 (2019).
[43] Q. Zhu, X. Li, and W. Lin, Leveraging neural differential equations and adaptive delayed feedback to detect unstable periodic orbits based on irregularly sampled time series, Chaos **33**, 031101 (2023).